An Optimization Strategy for Unit Commitment in High Wind Power Penetration Power Systems Considering Demand Response and Frequency Stability Constraints

Minhui Qian [1,2], Jiachen Wang [3], Dejian Yang [3,*], Hongqiao Yin [4] and Jiansheng Zhang [1]

1   College of Electrical and Power Engineering, Taiyuan University of Technology, Taiyuan 030024, China; minhui_qian@163.com (M.Q.); zhang-jsh@tsinghua.edu.cn (J.Z.)
2   National Key Laboratory of Renewable Energy Grid-Integration, China Electric Power Research Institute, Beijing 100192, China
3   School of Electrical Engineering, Northeast Electric Power University, Jilin 132012, China; wjc875195085@163.com
4   School of Electrical Engineering, Southeast University, Nanjing 210003, China; hongqiao_yin@seu.edu.cn
*   Correspondence: yangdejian@neepu.edu.cn

Abstract: To address the issue of accommodating large-scale wind power integration into the grid, a unit commitment model for power systems based on an improved binary particle swarm optimization algorithm is proposed, considering frequency constraints and demand response (DR). First, incentive-based DR and price-based DR are introduced to enhance the flexibility of the demand side. To ensure the system can provide frequency support, the unit commitment model incorporates constraints such as the rate of change of frequency, frequency nadir, steady-state frequency deviation, and fast frequency response. Next, for the unit commitment planning problem, the binary particle swarm optimization algorithm is employed to solve the mixed nonlinear programming model of unit commitment, thus obtaining the minimum operating cost. The results show that after considering DR, the load becomes smoother compared to the scenario without DR participation, the overall level of load power is lower, and the frequency meets the safety constraint requirements. The results indicate that a comparative analysis of unit commitment in power systems under different scenarios verifies that DR can promote rational allocation of electricity load by users, thereby improving the operational flexibility and economic efficiency of the power system. In addition, the frequency variation considering frequency safety constraints has also been significantly improved. The improved binary particle swarm optimization algorithm has promising application prospects in solving the accommodation problem brought by large-scale wind power integration.

Keywords: unit commitment; demand-side response; frequency security constraints; operational flexibility

1. Introduction

Under the context of carbon peaking and carbon neutrality goals and the accelerated construction of a secure and efficient new energy system, China's renewable energy industry has been developing rapidly [1]. In the process of building a new power system, the output of renewable energy sources is continuously rising [2]. However, the volatility of new energy increases the uncontrollability on the generation side and continuously reduces system inertia, leading to a higher likelihood of grid frequency exceeding allowable limits during disturbances [3]. As the share of thermal power units in the power system decreases, system inertia reduces, which in turn weakens the grid's frequency regulation capability, causing frequency drops and potentially leading to low-frequency load shedding or even system instability [4]. Therefore, in the operation of power systems, it is crucial to fully consider uncertainties and prioritize frequency security to avoid large-scale blackouts.

To address uncertainties on the load side, demand-side response (DSR) is gradually being promoted. The implementation of DSR can effectively enhance the security and economy of grid operation, preventing a decline in the efficiency of the electricity market [5,6]. Accurately, quickly, and efficiently tapping into the demand-side response potential is a key measure to alleviate supply pressure during peak periods and ensure the safe operation of the grid. At present, DSR has already been applied in electricity markets [7]. The specific forms of DSR include time-of-use pricing, which encourages users to adjust their electricity consumption periods autonomously [8], known as price-based demand response (PDR), or providing economic compensation to reduce electricity loads during specific periods [9], known as incentive-based demand response (IDR) [10]. There are two main types of research on incentive-based demand response: one focuses on decision-making optimization with bidding as the objective, and the other optimizes the control strategies of user electricity behavior [11]. Reference [12] proposes a standby scheduling model including demand response (DR), which improves the flexibility of system operation through DR. In reference [13], a multi-period electricity price response model is established, and the hybrid model is solved by the improved sparrow algorithm. Reference [14] puts forward the optimal scheduling based on DR, which improves the system's ability to absorb new energy. Reference [15] studies the respective applicable scenarios of PDR and IDR, which can improve the operational flexibility. It can be seen that the research on DR's participation in power grid dispatching has made remarkable progress, but the impact of DR on power system operation risk and economy has not been quantitatively analyzed in the above-mentioned existing reference research. How to realize the optimal operation of various units in the power system, improve the absorptive capacity of renewable energy in the power system, and realize the power balance of large-scale power grids has become an urgent problem to be solved.

The frequency of the power system is a crucial parameter in grid operation. When there is a power shortage in the system, the frequency drops, potentially triggering low-frequency load shedding in generators, which may lead to blackouts. Frequency security can be measured by frequency indicators [16]. The rate of change of frequency (RoCoF), frequency nadir, steady-state frequency, and fast frequency response (FFR) can effectively reflect whether the frequency of the power system is in a safe and stable state. Currently, the existing wind power grid-connected units mainly focus on power distribution between thermal power and wind power units to maintain grid stability [17]. The frequency regulation task of the power system is still undertaken by thermal power units. Reference [18] analyzes the active reserve treatment and distribution when wind turbines are connected to the system. Reference [19] deduces the maximum constraint of frequency drop for the frequency response model and adds it to the unit commitment to solve it, which effectively improves the economy and stability of the system. Reference [20] adds the maximum frequency deviation constraint to promote thermal power units to participate in primary frequency regulation to ensure the frequency safety of the system. Reference [21] deduces the formula of steady-state frequency deviation of the system according to droop characteristics, and the fan acts as a load and does not participate in primary frequency regulation. Reference [22] puts forward the task of reserving reserve for thermal power units to provide primary frequency response (PFR) and does not involve the joint participation of wind turbines and thermal power units in PFR.

This paper proposes a unit commitment model for power systems that considers frequency constraints and DR, using an improved binary particle swarm optimization algorithm. First, two types of demand-side response mechanisms, incentive-based DSR and price-based DSR, are proposed. On this basis, constraints such as RoCoF, frequency nadir, steady-state frequency, and FFR are added to ensure that the system can support primary frequency regulation. Next, for solving the unit commitment problem, the improved binary particle swarm optimization algorithm is used to solve the mixed nonlinear programming model of unit commitment to obtain the optimal economic cost of the model. Finally, by comparing unit commitment in power systems under different scenarios, it is verified that

the implementation of demand-side response can encourage users to allocate their electricity loads more rationally, thereby enhancing the operational flexibility and economic efficiency of the power system. Additionally, frequency variations are significantly improved when frequency security constraints are considered.

2. Consideration of Demand Response and Frequency Security Constraint Mathematical Model

2.1. Demand-Side Response

As the difference between peak and off-peak load increases, the pressure on the power supply also rises. By implementing DSR, grid operating costs can be reduced, and system operational risks can be mitigated [9]. According to the different methods of demand-side response, loads can be categorized into fixed loads, price-based transferable loads, and incentive-based curtailable loads [10].

DR strategies not only help improve the economic benefits of the grid but also enhance the flexibility and sustainability of the power system. Through scientific and reasonable load classification and management, more efficient allocation of power resources can be achieved, ensuring stable operation and a reliable power supply for the power system.

2.1.1. Incentive-Based DR

IDR can be classified into incentive-based curtailable loads depending on the incentives. This paper studies incentive-based transferable loads, with the formula as in [23]:

$$C^{\mathrm{IDR}} = \sum_{b=1}^{N_B} \sum_{t=1}^{N_T} (C_{b,t}^{\mathrm{IDR}} L_{b,t}^{\mathrm{IDR}} + C_{b,t}^{\mathrm{s.IDR}} \Delta L_{b,t}^{\mathrm{IDR}}) \tag{1}$$

where C^{IDR} represents the response cost of IDR; $L_{b,t}^{\mathrm{IDR}}$ is the curtailable load capacity reserved by users for the power operator; $C_{b,t}^{\mathrm{IDR}}$ is the unit capacity cost of the curtailable load; $\Delta L_{b,t}^{\mathrm{IDR}}$ is the actual interrupted load power after the power operator issues an interruption command; $C_{b,t}^{\mathrm{s.IDR}}$ is the cost of the actual interrupted load.

2.1.2. Price-Based DR

Price elasticity of demand measures the degree to which consumers adjust their demand for a good or service when its price changes. Specifically, if consumers significantly adjust their demand in response to price changes, the price elasticity of that good or service is considered high; conversely, if the change in demand is small, the price elasticity is considered low. In this paper, PDR focuses on transferable loads based on electricity pricing. The power load after PDR implementation is represented by the following equations [24]:

$$L = L^0 + \Delta L^{\mathrm{PDR}} \tag{2}$$

$$\Delta L_{NOR}^{\mathrm{PDR}} = E \times \Delta P_{\mathrm{NOR}} \tag{3}$$

$$L = \left[L_{b,1}, L_{b,2}, \cdots\cdots, L_{b,N_T} \right]^T \tag{4}$$

$$L^0 = \left[L_{b,1}^0, L_{b,2}^0, \cdots\cdots, L_{b,N_T}^0 \right]^T \tag{5}$$

$$\Delta L^{\mathrm{PDR}} = \left[\Delta L_{b,1}^{\mathrm{PDR}}, \Delta L_{b,2}^{\mathrm{PDR}}, \cdots\cdots, \Delta L_{b,N_T}^{\mathrm{PDR}} \right]^T \tag{6}$$

$$\Delta L_{\mathrm{NOR}}^{\mathrm{PDR}} = \left[\frac{\Delta L_{b,1}^{\mathrm{PDR}}}{L_{b,1}^0}, \frac{\Delta L_{b,2}^{\mathrm{PDR}}}{L_{b,2}^0}, \cdots\cdots, \frac{\Delta L_{b,N_T}^{\mathrm{PDR}}}{L_{b,N_T}^0} \right]^T \tag{7}$$

$$\Delta p_{\mathrm{NOR}} = \left[\frac{\Delta p_{b,1}}{p_{b,1}^0}, \frac{\Delta p_{b,2}}{p_{b,2}^0}, \cdots\cdots, \frac{\Delta p_{b,N_T}}{p_{b,N_T}^0} \right]^T \tag{8}$$

$$E_{mn} = \frac{\Delta L_{b,m}^{\text{PDR}}}{L_{b,m}^0} \Big/ \frac{\Delta p_{b,n}}{P_{b,n}^0} \tag{9}$$

$$C^{\text{PDR}} = C_{z,t} L_{z,t} + C_{z,t}^{\text{s}} \Delta L_{z,t} \tag{10}$$

where ΔL^{PDR} represents the matrix of price changes and load changes resulting from PDR implementation; E is the price elasticity matrix, with a size of $N_{\text{T}} \times N_{\text{T}}$; $L_z^{z,t}$ is the load transfer amount; $C_{z,t}$ is the unit capacity cost of the load transfer; $\Delta L_{z,t}$ is the transferred load power; $C_{z,t}^S$ is the cost of the load transfer.

2.2. Frequency Regulation Constraints for Wind and Thermal Units

During the dynamic changes in frequency, four key indicators are the rate of change of frequency, the frequency nadir, the steady-state frequency, and the fast frequency response. When the system's rate of change of frequency and fast frequency response exceed the specified limits, it exacerbates the frequency decline. If the frequency nadir and steady-state frequency also exceed the limits, large-scale blackouts may occur. Therefore, in unit commitment, it is necessary to consider constraints such as the rate of change of frequency, frequency nadir, steady-state frequency, and fast frequency response. By incorporating these frequency constraints, the unit startup/shutdown and power allocation can be optimized to maintain stable system operation under various load conditions. This also enhances the frequency stability and reliability of the system. These measures allow the power system to maintain stability more effectively during frequency fluctuations, ensuring safe operation.

Since both thermal and wind units provide PFR, H^* is given by [25]

$$H^* = \frac{\sum\limits_{i=1}^{N} H_i P_{i,\max} u_{i,t} + \sum\limits_{w=1}^{W} H_w W_{\text{f},t}}{P_{i,\max} u_{i,t} + W_{\text{f},t}} \tag{11}$$

where H_i and H_w are the time constants for thermal unit i and wind unit w, respectively; N is the number of thermal units; W is the number of wind turbines; $u_{i,t}$ is the on/off status of unit i at time t; and $W_{\text{f},t}$ is the predicted wind power.

The RoCoF constraint is given

$$\sum\limits_{w=1}^{W} \sum\limits_{i=1}^{N} (u_{i,t} H_i P_{i,\max} + H_w W_{\text{f},t}) \geqslant \left| \frac{\Delta P_{\text{L}} f_0}{2 F_{\max}} \right| \tag{12}$$

where ΔP_{L} is the load disturbance; $F_{\max}$ is the maximum allowed rate of change of frequency; and f_0 is the nominal grid frequency.

The frequency nadir constraint is given as in [25], as

$$\frac{\Delta P_{\text{L}}}{k_{\text{D}}} + \frac{2 H^* \Delta P_{\text{a}}}{T_{\text{d}} k_{\text{D}}^2} \ln \frac{2 H^* \Delta P_{\text{a}}}{2 H^* \Delta P_{\text{a}} + T_{\text{d}} (k_{\text{D}} \Delta P_{\text{L}} - k_{\text{D}}^2 \Delta f_{\text{DB}})} \leqslant \Delta f_{\max s} \tag{13}$$

where ΔP_{a} is the total incremental power; k_{D} is the damping coefficient; T_{d} is the cut-off time; Δf_{DB} is the cut-off frequency; and $\Delta f_{\max s}$ is the maximum allowed frequency drop.

The steady-state frequency constraint is

$$\Delta P_{\text{a}} \geqslant \Delta P_{\text{L}} - k_{\text{D}} \Delta f_{\max,\text{ss}} \tag{14}$$

where $\Delta f_{\max,\text{ss}}$ is the maximum allowed steady-state frequency variation.

The incremental power of the FFR constraint is

$$0 \leqslant \Delta P_{ai,t} \leqslant \Delta P_{ai,\max} \tag{15}$$

where $\Delta P_{ai,t}$ is the incremental power of FFR, and $\Delta P_{ai,\max}$ is the maximum incremental power of FFR.

3. Unit Commitment Model Considering DR and Dynamic Frequency Constraints

The unit commitment optimization model involving wind power is mainly composed of objective function and constraint conditions. In order to ensure that wind power can participate in frequency modulation, it is necessary to increase the constraint of wind-fire joint participation in frequency modulation, so as to construct a unit commitment optimization model including wind turbines participating in frequency modulation.

3.1. Objective Function

With the continuous improvement of wind power permeability, in order to ensure the stability of the power grid, this model aims at minimizing the power generation operation cost of the system and constructs a unit commitment optimization model. The improved binary particle swarm optimization algorithm is used to solve the unit commitment problem to achieve the optimization goal, which can ensure the safe operation of the power grid and maximize the economy of wind power.

In the recent stage, the deterministic scheduling and the predicted value of new energy are used to minimize the operation cost and ensure that the scheme meets the requirements of frequency stability. The objective function of the model is as follows [26].

$$
\begin{aligned}
\min C = & \sum_{i=1}^{N_G} \sum_{t=1}^{N_T} (f(P_{i,t}) + C_i^{\text{open}} u_{i,t} + C_i^{\text{close}}(1 - u_{i,t}) + \\
& C_R R_{i,t}) + \sum_{t=1}^{N_T} (C_{b,t}^{\text{IDR}} L_{b,t}^{\text{IDR}} + C_{b,t}^{\text{s.IDR}} \Delta L_{b,t}^{\text{IDR}} \\
& + C_{z,t} L_{z,t} + C_{z,t}^{\text{s}} \Delta L_{z,t}) + \sum_{w=1}^{N_W} \sum_{t=1}^{N_T} C^{\text{cur}} V_{w,t}
\end{aligned}
\tag{16}
$$

where N_G, N_W, and N_T represent the number of thermal units, wind farms, and time periods, respectively; $f(P_{i,t})$ is the fuel cost function for unit i; $P_{i,t}$ is the output of unit i at time t; $u_{i,t}$ is the on/off status of unit i at time t (where $u_{i,t} = 1$ indicates the unit is on and $u_{i,t} = 0$ indicates it is off); C_i^{open} and C_i^{close} are the startup and shutdown costs for unit i; $R_{i,t}$ is the reserve capacity of thermal unit i; C_R is the reserve cost; C^{cur} is the wind curtailment penalty coefficient; and $V_{w,t}$ is the curtailed wind power at time t.

3.1.1. Unit Operating Costs

Equation (17) provides the operating cost of the unit combination.

$$
f(P_{i,t}) = \alpha_{1,i} u_{i,t} + \alpha_{2,i} P_{i,t} + \alpha_{3,i} (P_{i,t})^2
\tag{17}
$$

where $\alpha_{1,i}$, $\alpha_{2,i}$, and $\alpha_{3,i}$ are the parameters for each term.

3.1.2. Unit Startup/Shutdown Constraints

Equation (18) provides the constraints for starting and stopping the unit combination.

$$
\begin{cases}
\sum\limits_{k=t}^{t+T_{\text{on},i}-1} u_{i,k} \geqslant T_{\text{on},i}(u_{i,t} - u_{i,t-1}) \\
\sum\limits_{k=t}^{t+T_{\text{off},i}-1} (1 - u_{i,k}) \geqslant T_{\text{off},i}(u_{i,t-1} - u_{i,t})
\end{cases}
\tag{18}
$$

where $T_{\text{on},i}$ and $T_{\text{off},i}$ are the minimum startup and shutdown times for unit i.

3.1.3. Unit Ramp Rate Constraints

Equation (19) provides the climbing constraint for the unit combination.

$$
\begin{cases}
P_{i,t} - P_{i,t-1} \leqslant UR_i \\
P_{i,t} - P_{i,t-1} \geqslant -DR_i
\end{cases}
\tag{19}
$$

where UR_i and DR_i are the maximum and minimum ramp rates of unit i, respectively.

3.1.4. Wind Power Integration Constraints

Equation (20) provides the constraint on wind power output.

$$0 \leqslant P_{w,t} \leqslant A_{w,t} \tag{20}$$

where $P_{w,t}$ is the grid-connected power at time t, and $A_{w,t}$ is the predicted power at time t.

3.1.5. Power Balance Constraints

Equation (21) provides the power balance constraint.

$$\sum_{i \in G_b} P_{i,t} + \sum_{w \in W_b} P_{w,t} = L_{b,t} + \Delta L_{b,t}^{\text{PDR}} - \Delta L_{b,t}^{\text{IDR}} \tag{21}$$

where $L_{b,t}$ represents the load power at time t; $\Delta L_{b,t}^{\text{PDR}}$ is the load change at time t; and $\Delta L_{b,t}^{\text{IDR}}$ is the curtailable demand response power.

3.1.6. DR Constraints

Equations (22)–(26) provide DR constraints.

$$0 \leqslant \Delta L_{b,t}^{\text{IDR}} \leqslant L_{b,t}^{\text{IDR}} \tag{22}$$

$$L_{b,t}^{\text{IDR}} \leqslant L_{b,t}^{\text{IDR,max}} \tag{23}$$

$$\Delta L^{\text{PDR}} = E' \Delta p \tag{24}$$

$$0 \leqslant \Delta L_{b,t}^{\text{PDR}} \leqslant L_{b,t}^{\text{PDR,max}} \tag{25}$$

$$0 \leqslant \Delta p_{b,t} \leqslant \Delta p_{b,t}^{\text{max}} \tag{26}$$

where $L_{b,t}^{\text{IDR,max}}$ and $L_{b,t}^{\text{PDR,max}}$ are the upper limits of load power for the two types of demand response, respectively; $\Delta p_{b,t}$ is the price change at time t; and $\Delta p_{b,t}^{\text{max}}$ is the upper limit of the price change at time t.

3.2. PLBPSO Algorithm

With the development of particle swarm optimization (PSO) [27], a binary particle swarm optimization (BPSO) algorithm has been derived for solving discrete optimization problems. BPSO is specifically designed for discrete optimization, showing greater adaptability. At the same time, the priority list (PL) method sorts schedulable units in the system based on their economic characteristics and adjusts the unit's dispatch according to the system's load conditions.

This paper first obtains an initial unit commitment plan, then generates an optimization window. The BPSO algorithm is applied within the optimization window for further solving and optimization. The optimization window is shown in Figure 1.

The improved algorithm first determines the base load units. Next, startup and shutdown adjustments are made to meet reserve operation requirements. After this process, the startup and shutdown plans for all periods satisfy the minimum startup/shutdown time constraints.
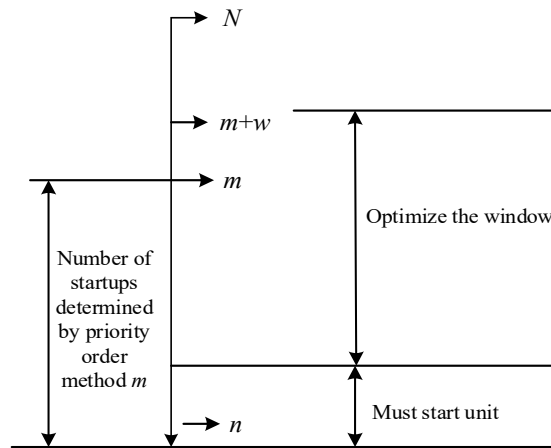
Figure 1. Optimization strategy.

3.3. Load Distribution Strategy

Figure 2 shows the flowchart of the economic load distribution problem. In addressing this issue, the equal incremental rate method based on the Lagrange multiplier method is used, combined with the bisection method for solving. ΔP represents the difference between the total output of the running units and the load.
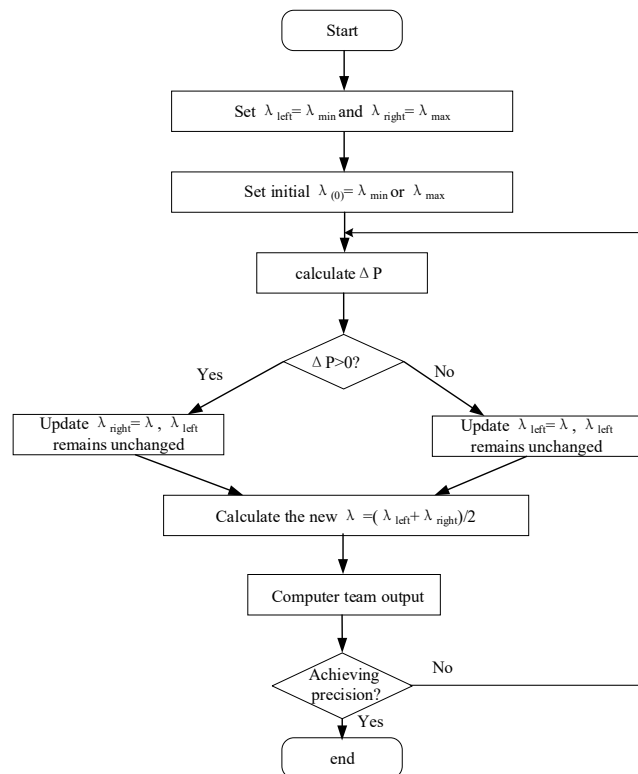

Figure 2. Economic load distribution process diagram.

Figure 3 shows the iterative steps of the PLBPSO algorithm. The process begins by setting the initial value of λ, with the left boundary set as $\lambda_{\min}$ and the right boundary set as $\lambda_{\max}$. The initial value of λ can be set to $\lambda_{\min}$ or $\lambda_{\max}$; next, by calculating the power difference ΔP, the sign of ΔP is checked. If ΔP is greater than 0, the right boundary value λ_{right} is updated to the current λ; if ΔP is less than or equal to 0, the left boundary value λ_{left} is updated to the current λ. Then, the new λ is set as the midpoint of the left and right boundaries, $\lambda = (\lambda_{\text{left}} + \lambda_{\text{right}})/2$. Based on the new λ, the unit output is calculated, and the

result is checked to see if it meets the set precision requirements. If the precision is met, the process ends; if not, the loop continues until the precision requirement is satisfied.
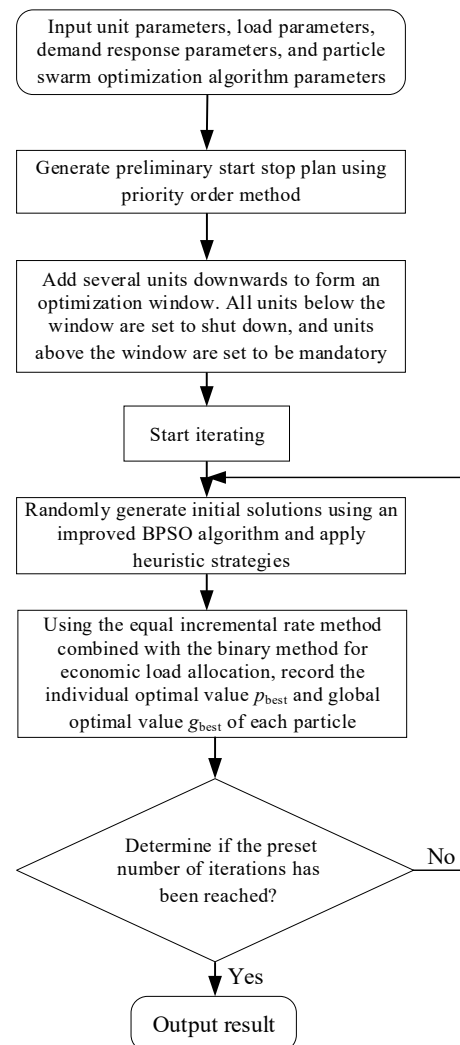

Figure 3. Algorithm iteration steps.

4. Case Study

In this paper, a case study is conducted on unit commitment in power systems under different scenarios. The programming was performed on the MATLAB R2022b platform, and the model was solved using an improved binary particle swarm optimization algorithm. The unit commitment in the power system is divided into two scenarios: Scenario 1, where unit commitment considers frequency security constraints but does not consider DSR; and Scenario 2, where unit commitment considers both frequency security constraints and DSR.

Figure 4 shows the wind power output and its predicted load over a day. The reference frequency is 50 Hz, the minimum frequency limit is 49.2 Hz, and the RoCoF limit is 0.5 Hz/s.

Based on (15), with the goal of minimizing comprehensive costs, considering the power regulation constraints of curtailable loads and transferable loads as well as system frequency constraints, the daily power curve and unit generation plan are obtained. The effectiveness of the proposed strategy is verified by comparing the results of load participation in DSR and the unit day-ahead scheduling plan.
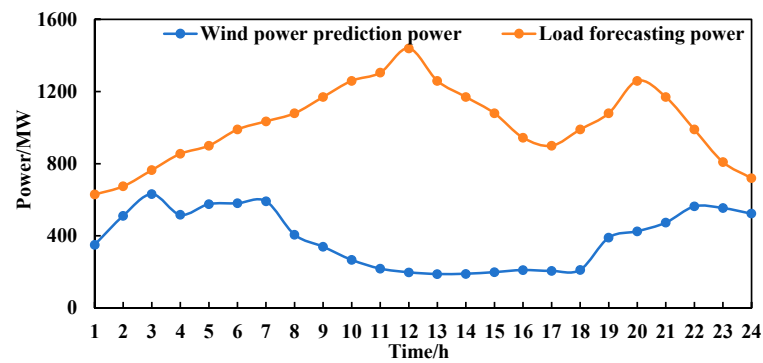
Figure 4. Wind and load forecasting power.

Figure 5 shows the power curves for curtailable loads and transferable loads participating in DSR. After participating in DSR, due to the influence of electricity prices, the final load curve during peak periods is lower than the initial load curve, and the changes in the load curve after DSR implementation have a positive impact on the stability and economy of the power system. The smoother load curve reduces the operational risk of the grid, decreases the need for frequent startup and shutdown of peaking plants, and thus lowers operating and maintenance costs. Moreover, the effective implementation of DSR also enhances user participation in grid regulation, laying a foundation for the development of future smart grids, demonstrating the effectiveness of DSR implementation.
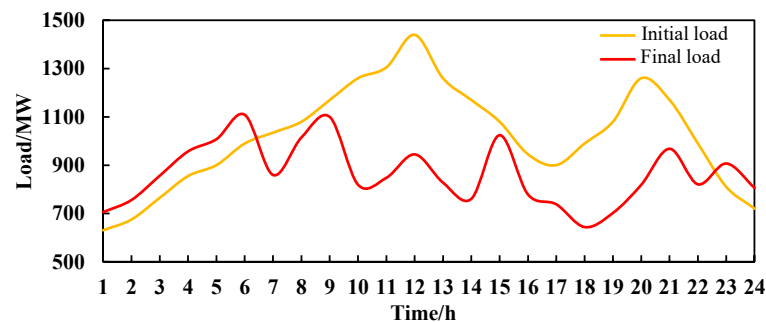
Figure 5. Load curve.

Figure 6 presents the time-of-use electricity price for a typical day. Through the dynamic adjustment mechanism of time-of-use pricing, the power system achieves a reasonable distribution of the load, significantly reducing peak loads and filling in valley loads, making the load curve smoother and system operation more stable. Additionally, this price adjustment mechanism improves the efficiency of the electricity market, and users responding to price signals enhance overall economic benefits.

Figure 7 presents the transferable load power after DSR implementation. Transferable load power is guided by time-of-use pricing and obtained based on power transfer constraints and transfer volume constraints over 24 h. From Figure 7, it can be observed that during peak periods, transferable power is around 150 MW, effectively addressing the load demand during peak periods. During off-peak periods, transferable load power can be dispatched to meet the remaining load demand, indicating that by appropriately increasing the power consumption of transferable loads during periods of low power demand, not only can equipment utilization be improved, but power resource waste can also be avoided, further balancing the grid load curve and fully demonstrating the importance of DSR in optimizing power system operation.
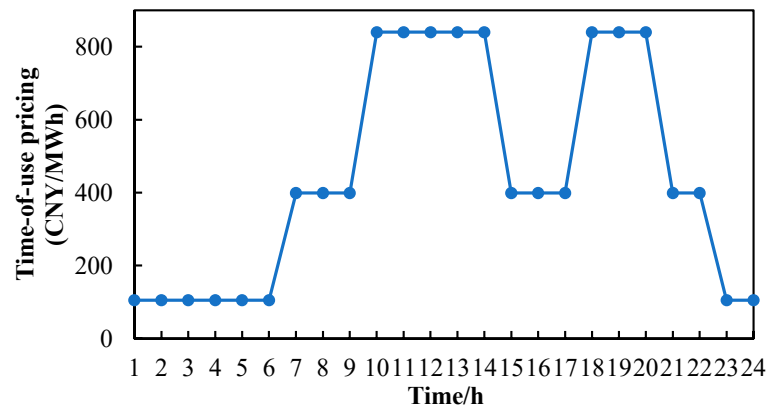
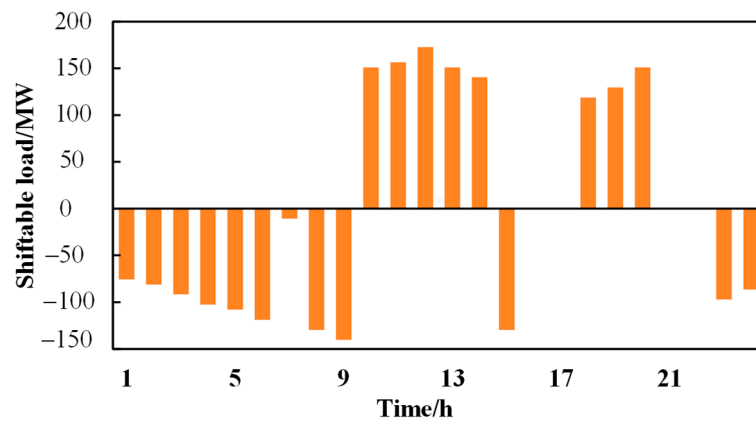**Figure 6.** Time-of-use electricity price in each period of a day.

Figure 7. Shiftable load power curve.

Figure 8 shows the curtailable load power reflected by the first, second, and third levels of load after DSR implementation. Curtailable load power is calculated through constraints on the interruption of various load levels and the continuity of curtailable loads. Guided by DSR, the phenomenon of large load fluctuations can be effectively mitigated. From Figure 8, it can be seen that during peak periods, the curtailable load power for the first, second, and third levels is at its peak; during off-peak periods, such as from midnight to 6 AM, the first, second, and third levels do not need to interrupt their loads. Through the implementation of the DSR strategy and proper management of curtailable loads, non-critical loads can be effectively interrupted during peak periods, significantly reducing power demand during these times, preventing grid overload and power shortages. During off-peak periods, normal load operation is maintained, improving the efficiency of power resource utilization and preventing power waste.
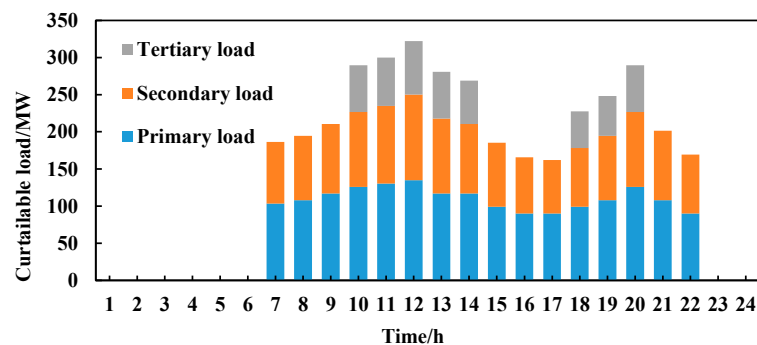

Figure 8. Curtailable load power curve.

Figure 9 shows the comparison of the iterative performance between the BLBPSO algorithm used in this paper and the traditional PSO algorithm. The BLBPSO algorithm accelerates the exploration speed of particles in the solution space and enhances the global search capability by introducing boundary constraints and improved adaptive strategies. From the figure, it can be seen that compared to traditional particle swarm optimization algorithms, BLBPSO improves convergence speed and search efficiency while ensuring that the system achieves optimality.
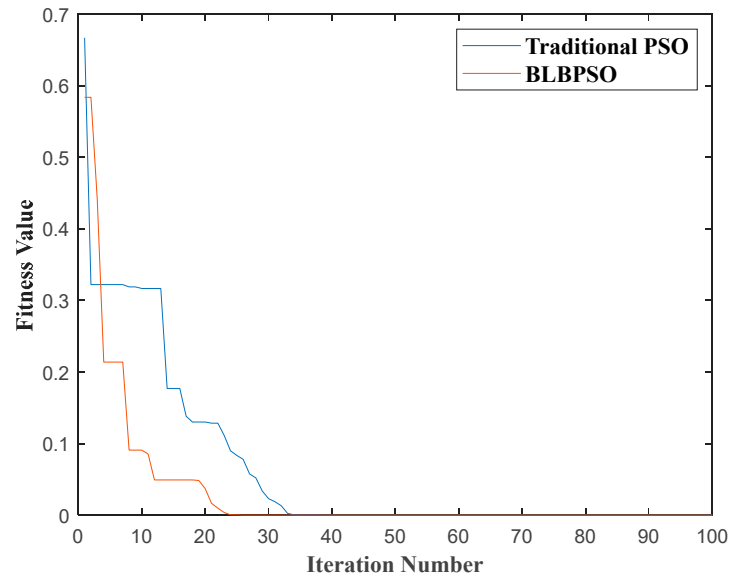
Figure 9. Comparison of iterative effects of different algorithms.

Figures 10 and 11 present the unit commitment outputs under different scenarios. By superimposing transferable and curtailable loads, the load curve after DSR is obtained, and then, through unit commitment, the day-ahead scheduling of load power before and after DSR participation is conducted, resulting in the unit commitment output under different scenarios. From Figures 10 and 11, it can be seen that the load in Scenario 2 is smoother and lower than in Scenario 1. After DSR implementation, the unit commitment of the power system effectively enhances system operational flexibility, reduces operational risks, and enables the system to respond more effectively to load changes, quickly adjusting unit output to maintain the supply–demand balance. This flexibility not only improves the system's ability to cope with sudden load changes but also enhances system stability and reliability under different operating conditions.
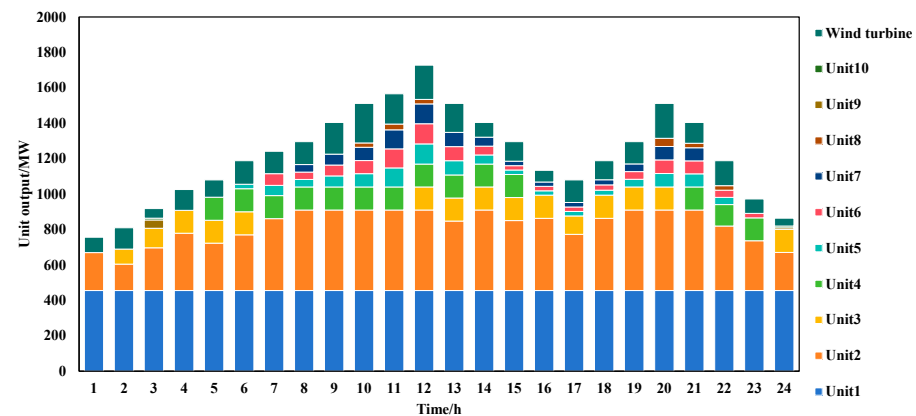

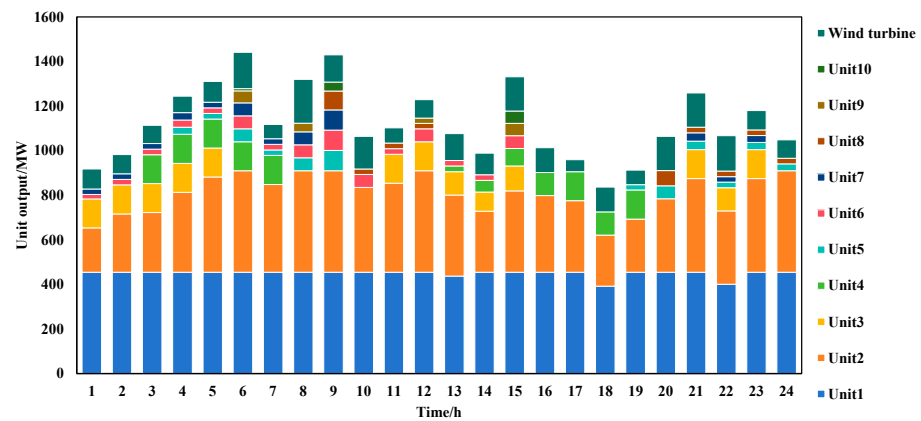**Figure 10.** Scenario 1 unit combination output.

Figure 11. Scenario 2 unit combination output.

Table 1 presents the frequency change results under different scenarios. From the table, it can be seen that under different scenarios with frequency security constraints considered, the frequency meets the safety constraint requirements. The four indicators of the system's rate of change of frequency, frequency nadir, steady-state frequency, and fast response frequency are significantly improved, enhancing system stability.

Table 1. Frequency changes in different scenarios.

Time/h	Scena. 1	Scena. 2	Time/h	Scena. 1	Scena. 2
1	50.000	50.000	13	49.973	49.973
2	49.934	49.934	14	49.973	49.958
3	49.921	49.921	15	49.972	49.957
4	49.921	49.921	16	49.970	49.956
5	49.914	49.927	17	49.971	49.956
6	49.914	49.927	18	49.955	49.970
7	49.925	49.913	19	49.935	49.949
8	49.933	49.933	20	49.931	49.931
9	49.954	49.94	21	49.939	49.925
10	49.949	49.963	22	49.929	49.993
11	49.969	49.970	23	49.930	49.930
12	49.957	49.972	24	49.933	49.934

Table 2 presents the costs required for unit commitment under different scenarios. It shows that the total cost in Scenario 2 is reduced by CNY 83,600 compared to Scenario 1, a 1.4% decrease. The thermal unit output cost is reduced by CNY 608,500 yuan, a 13.9% decrease, and the reserve cost of thermal units is reduced by CNY 135,100, a 14.6% decrease. The reason is that in Scenario 2, the load curve decreases after DSR, leading to a reduction in the various costs of thermal units. Although the costs of curtailable and transferable loads increase, the total cost still shows a decreasing trend. The results indicate that DSR measures have a significant effect on optimizing load distribution and reducing the total cost of the power system. Through reasonable load management, the power system can not only achieve economic operation but also improve operational efficiency and stability. The application of DSR strategies allows the power system to respond more flexibly to load changes, reducing the pressure of peak loads on the system, optimizing resource allocation, and improving overall economic efficiency.

Table 2. Cost results under different scenarios.

	Scena. 1	Scena. 2
Output cost of thermal power unit/CNY 10,000	436.25	375.40
Standby cost of thermal power unit/CNY 10,000	92.59	79.08
Penalty cost for abandoning wind/CNY 10,000	64.71	59.73
Curtailable load cost/CNY 10,000	0	61.61
Transferable load cost/CNY 10,000	0	9.37
Total cost/CNY 10,000	593.55	585.19

5. Results Discussion

In the study of power system unit commitment, this paper optimizes the unit commitment of the power system by considering frequency security constraints and DSR. In terms of frequency, this paper imposes constraints on four key indicators: the rate of change of frequency, the frequency nadir, the steady-state frequency, and the fast frequency response, to ensure that the power system can effectively maintain stability and operate safely, with the final frequencies meeting the safety constraint requirements. In terms of DSR, this paper employs a method in which loads participate in DSR, fully considering the parameters and constraints after DSR implementation. After DSR implementation, the unit commitment of the power system can effectively enhance system operational flexibility, reduce operational risks, and enable the system to respond more effectively to load changes. This allows the system to quickly adjust unit output and maintain the supply–demand balance through reasonable load management and scheduling.

Based on a thorough analysis of the operating conditions of unit commitment, this paper proposes a power system unit commitment model that considers frequency security constraints and DSR. Compared to thermal unit commitment, the proposed model focuses more on the safe and stable operation of the power system and optimized scheduling, using load data from a typical day to drive the reasonable allocation of generation plans. The calculation results show that in Scenario 2, the total cost is reduced by CNY 83,600 compared to Scenario 1; the thermal unit output cost is reduced by CNY 608,500; and the thermal unit reserve cost is reduced by CNY 135,100. This indicates that the proposed method has significant advantages in optimizing unit commitment scheduling. The results demonstrate that the proposed model not only improves the stability and flexibility of the system but also reduces the cost of unit commitment. This allows the power system to respond more flexibly to load changes, reduces the pressure of peak loads on the system, optimizes resource allocation, and improves overall economic efficiency.

Although positive results were achieved, there are still some limitations. This paper considers the load data of a typical day, but the load power data for the entire year were not collected in detail for the study. Therefore, the model was not optimized and scheduled using annual unit operation data. In future research, more comprehensive load data can be collected to validate and optimize the model further.

6. Conclusions

This paper develops a power system unit commitment model that considers frequency security constraints and DSR, based on an improved binary particle swarm optimization algorithm. Case study simulation was conducted, and the following conclusions were drawn:

(1) By incorporating frequency security constraints into the optimization model, the frequency fluctuations of the system can be significantly improved, enhancing the overall system stability.
(2) Load participation in DSR allows for rational adjustments to users' electricity consumption periods, improving the operational flexibility of the power system while reducing operational risks.

(3) The power system unit commitment method, which comprehensively considers frequency security constraints and DSR, not only improves system stability and flexibility but also reduces the cost of unit commitment.

Future research will strive to take setup, operational, and maintenance costs into account to achieve a more comprehensive cost–benefit analysis. In addition, the optimal UC strategy would be addressed considering more generating units to improve the flexibility of power systems integrated with high renewable energy.

References

1. Yang, Y.; Peng, J.C.H.; Ye, C.; Ye, Z.S.; Ding, Y. A criterion and stochastic unit commitment towards frequency resilience of power systems. *IEEE Trans. Power Syst.* **2022**, *37*, 640–652. [CrossRef]
2. Chu, Z.; Markovic, U.; Hug, G.; Teng, F. Towards optimal system scheduling with synthetic inertia provision from wind turbines. *IEEE Trans. Power Syst.* **2020**, *35*, 4056–4066. [CrossRef]
3. Zhu, D.; Wang, Z.; Hu, J.; Zou, X.; Kang, Y.; Guerrero, J.M. Rethinking Fault Ride-Through Control of DFIG-Based Wind Turbines From New Perspective of Rotor-Port Impedance Characteristics. *IEEE Trans. Sustain. Energy* **2024**, *15*, 2050–2062. [CrossRef]
4. Yang, D.; Li, J.; Jin, Z.; Yan, G.; Wang, X.; Ding, L.; Zhang, F.; Terzija, V. Sequential Frequency Regulation Strategy for DFIG and Battery Energy Storage System Considering Artificial Deadbands. *Int. J. Electr. Power Energy Syst.* **2024**, *155*, 109503. [CrossRef]
5. Wang, Y.; Wang, Y.; Huang, Y.; Yang, J.; Ma, Y.; Yu, H.; Zeng, M.; Zhang, F.; Zhang, Y. Operation optimization of regional integrated energy system based on the modeling of electricity-thermal-natural gas network. *Appl. Energy* **2019**, *251*, 113410. [CrossRef]
6. Baroche, T.; Pinson, P.; Latimier, R.L.G.; Ben Ahmed, H. Exogenous cost allocation in peer-to-peer electricity markets. *IEEE Trans. Power Syst.* **2019**, *34*, 2553–2564. [CrossRef]
7. Zhang, X.; Chan, K.W.; Wang, H.; Hu, J.; Zhou, B.; Zhang, Y.; Qiu, J. Game-theoretic planning for integrated energy system with independent participants considering ancillary services of power-to-gas stations. *Energy* **2019**, *176*, 249–264. [CrossRef]
8. Wu, L.; Shahidehpour, M.; Li, Z. Comparison of scenario-based and interval optimization approaches to stochastic SCUC. *IEEE Trans. Power Syst.* **2012**, *27*, 913–921. [CrossRef]
9. Han, K.-H.; Kim, J.-H. Genetic quantum algorithm and its application to combinatorial optimization problem. In Proceedings of the IEEE International Conference on Evolutionary Computation, La Jolla, CA, USA, 16–19 July 2000; pp. 1354–1360.
10. Yuan, X.; Chen, R.; Wang, Y. Two-stage robust unit commitment with frequency constraints considering risk and demand response. *Power Syst. Big Data* **2022**, *25*, 17–25.
11. Sun, Q.; Wu, Z.; Ma, Z.; Gu, W.; Zhang, X.-P.; Lu, Y.; Liu, P. Resilience enhancement strategy for multi-energy systems considering multi-stage recovery process and multi-energy coordination. *Energy* **2022**, *241*, 122834. [CrossRef]
12. Liu, X.; Wang, B.; Li, Y.; Wang, K. Stochastic unit commitment model for high wind power integration considering demand side resources. *Proc. CSEE* **2015**, *35*, 3714–3723.
13. Chen, Z.; Zhang, Y.; Ma, G.; Guo, C.; Zhang, J. Two-stage day-ahead and intra-day robust reserve optimization considering demand response. *Autom. Electr. Power Syst.* **2019**, *43*, 67–76.
14. Chen, Q.; Wang, W.; Wang, H. Bi-level optimization model of an active distribution network based on demand response. *Power Syst. Prot. Control* **2022**, *50*, 1–13.
15. Li, Z.; Wu, L.; Xu, Y.; Wang, L.; Yang, N. Distributed tri-layer risk-averse stochastic game approach for energy trading among multi-energy microgrids. *Appl. Energ.* **2023**, *331*, 120282. [CrossRef]

16. Eto, J.H.; Undrill, J.; Mackin, P.; Daschmans, R.; Williams, B.; Haney, B.; Hunt, R.; Ellis, J.; Illian, H.; Martinez, C.; et al. *Use of Frequency Response Metrics to Assess the Planning and Operating Requirements for Reliable Integration of Variable Renewable Generation*; Lawrence Berkeley National Lab. (LBNL): Berkeley, CA, USA, 2017. [CrossRef]

17. Yang, D.; Wang, X.; Chen, W.; Yan, G. Adaptive Frequency Droop Feedback Control-Based Power Tracking Operation of a DFIG for Temporary Frequency Regulation. *IEEE Trans. Power Syst.* **2024**, *39*, 2682–2692. [CrossRef]

18. Paturet, M.; Markovic, U.; Delikaraoglou, S.; Vrettos, E.; Aristidou, P.; Hug, G. Stochastic unit commitment in low-inertia grids. *IEEE Trans. Power Syst.* **2020**, *35*, 3448–3458. [CrossRef]

19. Zhang, Z.; Du, E.; Teng, F.; Zhang, N.; Kang, C. Modeling frequency dynamics in unit commitment with a high share of renewable energy. *IEEE Trans. Power Syst.* **2020**, *35*, 4383–4395. [CrossRef]

20. Nguyen, N.; Almasabi, S.; Bera, A.; Mitra, J. Optimal power flow incorporating frequency security constraint. *IEEE Trans. Ind. Appl.* **2020**, *55*, 6508–6516. [CrossRef]

21. Münz, U.; Mešanović, A.; Metzger, M.; Wolfrum, P. Robust optimal dispatch, secondary, and primary reserve allocation for power systems with uncertain load and generation. *IEEE Trans. Control Syst. Technol.* **2018**, *26*, 475–485. [CrossRef]

22. Ge, X.; Zhu, X.; Fu, Y.; Xu, Y.; Huang, L. Optimization of Reserve With Different Time Scales for Wind-Thermal Power Optimal Scheduling Considering Dynamic Deloading of Wind Turbines. *IEEE Trans. Sustain. Energy* **2022**, *13*, 2041–2050. [CrossRef]

23. Tumuluru, V.K.; Huang, Z.; Tsang, D.H.K. Integrating Price Responsive Demand Into the Unit Commitment Problem. *IEEE Trans. Smart Grid* **2014**, *5*, 2757–2765. [CrossRef]

24. Ray, P.K.; Jena, C.J. Security-Constrained Unit Commitment for Demand Response Provider—A Stochastic Approach. In Proceedings of the 2020 IEEE International Conference on Power Electronics, Smart Grid and Renewable Energy (PESGRE2020), Cochin, India, 2–4 January 2020; pp. 1–5.

25. Zeng, Y.; Yu, Y.; Li, J.; Li, B.; Hu, Y.; Zhu, L. Frequency Dynamics-Constrained Unit Commitment with High Penetration of Wind Power. In Proceedings of the 2023 8th International Conference on Power and Renewable Energy (ICPRE), Shanghai, China, 22–25 September 2023; pp. 1986–1991.

26. Aoyagi, H.; Chakraborty, S.; Mandal, P.; Shigenobu, R.; Conteh, A.; Senjyu, T. Unit Commitment Considering Uncertainty of Price-Based Demand Response. In Proceedings of the 2018 IEEE PES Asia-Pacific Power and Energy Engineering Conference (APPEEC), Kota Kinabalu, Malaysia, 7–10 October 2018; pp. 406–410.

27. Elsayed, W.; Hegazy, Y.G.; El-Bages, M.S.; Bendary, F.M. Improved random drift particle swarm optimization with self-adaptive mechanism for solving the power economic dispatch problem. *IEEE Trans. Ind. Inform.* **2017**, *13*, 1017–1026. [CrossRef]